Communication

UV–Vis Microspectroscopy: Probing the Initial Stages of Supported Metal Oxide Catalyst Preparation

Leon G. A. van de Water, Jaap A. Bergwerff, T. Alexander Nijhuis, Krijn P. de Jong, and Bert M. Weckhuysen

J. Am. Chem. Soc., **2005**, 127 (14), 5024-5025• DOI: 10.1021/ja044460u • Publication Date (Web): 17 March 2005

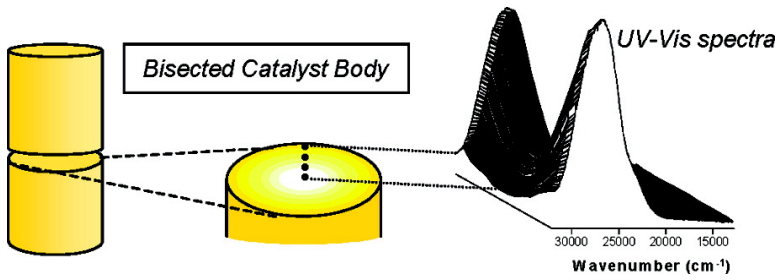

More About This Article

Additional resources and features associated with this article are available within the HTML version:

- Supporting Information
- Links to the 1 articles that cite this article, as of the time of this article download
- Access to high resolution figures
- Links to articles and content related to this article
- Copyright permission to reproduce figures and/or text from this article

View the Full Text HTML

J|A|C|S
COMMUNICATIONS

Published on Web 03/17/2005

UV−Vis Microspectroscopy: Probing the Initial Stages of Supported Metal Oxide Catalyst Preparation

Leon G. A. van de Water, Jaap A. Bergwerff, T. Alexander Nijhuis, Krijn P. de Jong, and Bert M. Weckhuysen*

Department of Inorganic Chemistry and Catalysis, Debye Institute, Utrecht University, P.O. Box 80083, 3508 TB Utrecht, The Netherlands

Received September 13, 2004; E-mail: B.M.Weckhuysen@chem.uu.nl

The need for catalysts with well-defined activity, selectivity, and stability is well recognized.[1] Rational design of improved catalysts requires a detailed understanding of the structure−function correlations of catalytic materials. Major advances in catalysis research are only to be expected when the detailed nature (i.e., on the molecular level) of the active species is known and the phenomena occurring upon synthesis fully understood. As such, the development of new synthetic strategies depends strongly on the emergence of advanced characterization techniques for these materials and preparation processes. The importance of the HRTEM technique for the understanding and subsequent fast development of the zeolite synthesis field illustrates this point.[2]

A large number of catalytic materials comprise metal (oxide) species supported onto oxidic supports, where the local molecular structure of the active component(s) and the macrodistribution over the support are important factors in terms of catalyst performance. Many of the phenomena occurring during catalyst preparation still defy thorough understanding.[3] This lack of fundamental understanding is the reason that improvements in the field of catalyst preparation are most often not based on mastering the chemical and physical processes occurring at multiple length scales, but, instead, are the result of long trial-and-error processes.

In this communication, we present a UV−vis microspectroscopy tool that enables monitoring, with a resolution of 100 μm or less, of the molecular structure of catalytically active components, along with their macrodistribution over support bodies. This study thus aims at investigating catalyst preparation at multiple length scales using UV−vis spectroscopy and is as such, to the best of our knowledge, the first of its kind. We will show that valuable additional information can be obtained, compared to conventional spectroscopic studies involving supported catalysts in powder form.[4] The UV−vis setup comprises a probe containing seven optical fibers, one connected to a light source and six to a spectrophotometer (Figure 1). Spatially resolved measurements are performed by remote-controlled automated stepwise motion of the measuring cell, containing a bisected catalyst body. The setup is designed for probing the metal−ion speciation of catalyst precursors along the cross-section of bisected millimeter-sized catalyst bodies, allowing the study of both the wet (i.e., impregnation) and the dry stages (drying, calcination) of the preparation process. To illustrate the broad range of catalytic systems for which this methodology may be applied to, two examples are presented here, including Ni ($d-d$ transition bands) on γ-Al_2O_3 and Cr (charge-transfer bands) on γ-Al_2O_3.

Ni^{2+} $d-d$ transition bands have been monitored qualitatively after pore−volume impregnation of γ-Al_2O_3 pellets ($\varnothing$ = 3 mm) with an acidified solution containing 0.5 M Ni^{2+} and 1.5 M ethylenediamine (*en*) (pH = 4.7). The UV−vis spectra, recorded 5 min after impregnation, are depicted in Figure 2 (top 5 traces). The spectrum of the impregnation solution (trace *I*) is included for reference purposes. The spectrum recorded near the edge of the cross-section (1500 μm) clearly resembles that of the solution. In contrast, the spectra recorded further toward the center of the pellet show a clear blue shift of the absorption bands; the ν_2 band is shifted from 15 400 cm^{-1} near the edge (1500 μm) to 17 400 cm^{-1} in the center of the pellet (0 μm), and the ν_3 band is shifted from 25 900 to 28 950 cm^{-1}. The shift of these bands is caused by changes in

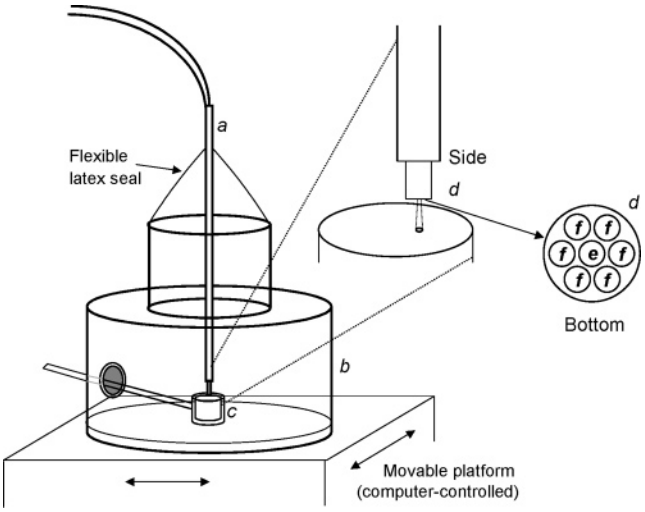

Figure 1. UV−vis DRS measuring cell. (a) UV−vis probe (fixed position); (b) closed glass cell containing a small amount of water to ensure a relative humidity of 100%; (c) sample holder; (d) UV−vis probe (enlarged) containing seven optical fibers ($\varnothing$ = 100 μm), connected either to the light source (e) or to the spectrophotometer (f).

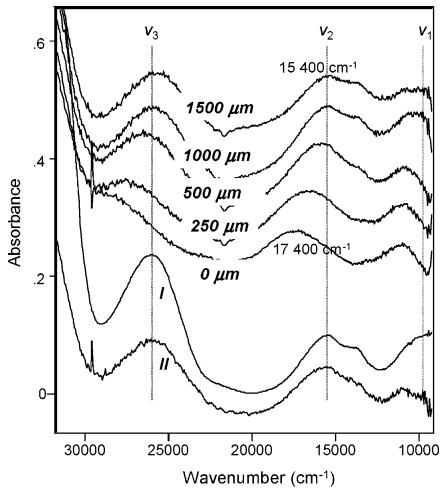

Figure 2. γ-Al_2O_3 pellets impregnated with 0.5 M $(Ni(NO_3)_2$ + 1.5 M *en* + HNO_3 (pH 4.7), 5 min after impregnation. The distance from the center of the pellet is indicated. (*I*) Impregnation solution; (*II*) impregnated powdered γ-Al_2O_3 sample.

10.1021/ja044460u CCC: $30.25

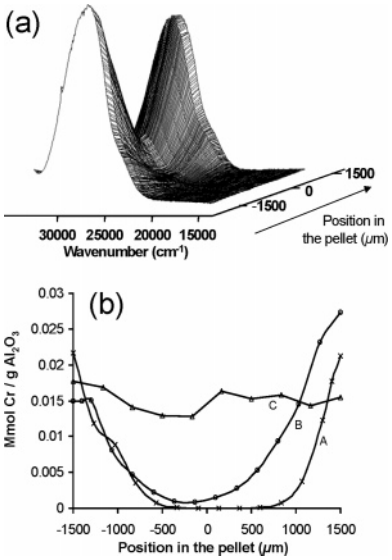

Figure 3. (a) UV−vis spectra recorded 6 h after impregnation of γ-Al_2O_3 pellets with a 0.01 M CrO_3 solution (pH 6.1) across the surface of a bisected support body. (b) CrO_4^{2-} concentration profiles inside γ-Al_2O_3 bodies at different points in time: (A) 2 h, (B) 6 h, and (C) 72 h after impregnation.

the coordination sphere of Ni^{2+} due to changes in the local pH upon diffusion of the acidic solution into basic γ-Al_2O_3. The *en* ligands are protonated in the impregnation solution and are not coordinated to Ni^{2+}. Toward the center of the γ-Al_2O_3 pellet, the pH increases, deprotonation of protonated *en* occurs, and water ligands are exchanged for *en*. By comparing the position of the UV absorption band in the center of the pellet (17 400 cm^{-1}) with that of spectra measured in solution at varying pH, the local pH in the center of the pellet was estimated to be ~6.2. Hence, the UV−vis spectra reveal detailed information not only on the distribution and local coordination environment of Ni^{2+} but also indirectly on the local pH value. Trace *II* in Figure 2 shows the UV−vis spectrum of a sample of crushed γ-Al_2O_3, 5 min after impregnation with the same solution. This spectrum can be regarded as the average spectrum of the spectra recorded across the cross-section and is very much solution-like. In other words, measurements on impregnated γ-Al_2O_3 powders do not reveal the detailed information on local differences inside catalyst support bodies during impregnation that can be obtained by analyzing bisected γ-Al_2O_3 catalyst bodies with the developed UV−vis optical fiber setup.

The transport of chromium oxide through γ-Al_2O_3 bodies after impregnation with a CrO_3 solution is a slow process. The UV−vis (DRS) spectra recorded 6 h after impregnation of γ-Al_2O_3 pellets with a 0.01 M CrO_3 solution (the pH adjusted to 6.1) show charge-transfer bands of chromate (CrO_4^{2-}) species, found at around 36 350 and 26 650 cm^{-1}.[5] In Figure 3a, the 26 650 cm^{-1} band is depicted at different positions across the surface of a bisected support body. The band positions do not shift throughout the pellet, indicating that no species other than CrO_4^{2-}, such as $Cr_2O_7^{2-}$ (which has an absorption band at 22 200 cm^{-1}), are present. To be able to quantify the CrO_4^{2-} distribution throughout the pellet, the charge-transfer band at 26 650 cm^{-1} was used to create a calibration curve. The CrO_4^{2-} concentration profiles at different points in time inside γ-Al_2O_3 bodies have been quantified using this calibration curve and are depicted in Figure 3b. After 2 h, a sharp drop in Cr concentration over the first 500 μm from the edge was observed. After 72 h, the CrO_4^{2-} distribution was found to have reached an equilibrium value close to the calculated 0.011 mmol Cr/g γ-Al_2O_3 (1.1 mL of the 0.01 M CrO_3 solution per gram of γ-Al_2O_3).

The spectroscopic information obtained with the optical fiber UV−vis setup presented here highlights the potential of this tool in probing the local metal−ion speciation throughout catalyst−support bodies in the early stages of catalyst preparation. The changes occurring to catalyst−precursor species during preparation are often a function of subtle changes in the ratio of different components, pH,[6] and reactivity of the support.[7] Until now, these phenomena inside catalyst bodies have not been described with spatial resolution, required in the quest for catalysts with narrowly defined properties. It is envisaged that UV−vis microspectroscopy may contribute toward a better understanding of the preparation process of supported catalysts, involving supports such as alumina and metal−oxide species with characteristic *d*−*d* or charge-transfer transitions. Moreover, a more detailed understanding of the preparation process of more complex catalysts, such as bimetallic (Co)-MoS_2−γ-Al_2O_3 catalysts, may be within reach. In certain cases, where the impregnated species do not change throughout the support body and over time, even quantitative analysis can be performed. When combined with spectroscopic studies on catalyst performance under reaction conditions,[8] the fate of a supported metal oxide may be studied throughout its whole life cycle. Finally, combining it with other local probing techniques, such as Raman microscopy,[9] may even further enhance the potential of this tool. UV−vis is complementary to Raman spectroscopy in cases where multiple species are present, such as Co and Mo, where Co^{2+} can be monitored with UV−vis and Mo^{6+} with Raman spectroscopy.

The analysis of (biological) microscopic samples, using FT infrared microspectroscopy with high spatial resolution (10−100 μm), is well documented.[10] In the future, UV−vis microspectroscopy may have potential toward applications different from heterogeneous catalysis, such as for biomedical and materials science purposes.

Acknowledgment. B.M.W. acknowledges NWO-CW for a VICI grant, whereas T.A.N. is grateful to a NWO-STW VIDI grant.

Supporting Information Available: Experimental details and synthetic method details (PDF). This material is available free of charge via the Internet at http://pubs.acs.org.

References

(1) (a) Fujdala, K. L.; Drake, I. J.; Bell, A. T.; Tilley, T. D. *J. Am. Chem. Soc.* **2004**, *126*, 10864−10866. (b) Fujdala, K. L.; Tilley, T. D. *J. Catal.* **2003**, *216*, 265−275. (c) Bell, A. T. *Science* **2003**, *299*, 1688−1691. (d) Schlögl, R.; Abd Hamid, S. B. *Angew. Chem., Int. Ed.* **2004**, *43*, 1628−1637. (e) de Jong, K. P. *Curr. Opin. Solid State Mater. Sci.* **1999**, *4*, 55−62.

(2) Thomas, J. M.; Terasaki, O.; Gai, P. L.; Zhou, W.; Gonzalez-Calbet, J. *Acc. Chem. Res.* **2001**, *34*, 583−594.

(3) (a) Neimark, A. V.; Kheifez, L. I.; Fenelonov, V. B. *Ind. Eng. Chem. Prod. Res. Dev.* **1981**, *20*, 439−450. (b) de Jong, K. P. *CatTech* **1998**, *3*, 87−95. (c) Lekhal, A.; Glasser, B. J.; Khinast, J. G. *Chem. Eng. Sci.* **2004**, *59*, 1063−1077.

(4) (a) Negrier, F.; Marceau, E.; Che, M. *Chem. Commun.* **2002**, 1194−1195. (b) d'Espinose de la Caillerie, J.-B.; Kermarec, M.; Clause, O. *J. Am. Chem. Soc.* **1995**, *117*, 11471−11481. (c) Brühwiler, D.; Frei, H. *J. Phys. Chem. B* **2003**, *107*, 8547−8556. (d) Carriat, J. Y.; Che, M.; Kermarec, M.; Verdaguer, M.; Michalowicz, A. *J. Am. Chem. Soc.* **1998**, *120*, 2059−2070.

(5) Weckhuysen, B. M.; Wachs, I. E.; Schoonheydt, R. A. *Chem. Rev.* **1996**, *96*, 3327−3349.

(6) Schreier, M.; Regalbuto, J. R. *J. Catal.* **2004**, *225*, 190−202.

(7) Carrier, X.; Lambert, J.-F.; Kuba, S.; Knözinger, H.; Che, M. *J. Mol. Struct.* **2003**, *656*, 231−238.

(8) (a) Weckhuysen, B. M. *Phys. Chem. Chem. Phys.* **2003**, *5*, 4351−4360. (b) Nijhuis, T. A.; Tinnemans, S. J.; Visser, T.; Weckhuysen, B. M. *Phys. Chem. Chem. Phys.* **2003**, *5*, 4361−4365.

(9) Bergwerff, J. A.; Visser, T.; Leliveld, B. R. G.; Rossenaar, B. D.; de Jong, K. P.; Weckhuysen, B. M. *J. Am. Chem. Soc.* **2004**, *126*, 14548−14556.

(10) (a) Wetzel, D. L.; LeVine, S. M. *Science* **1999**, *285*, 1224−1225. (b) Tobin, M. J.; Chesters, M. A.; Chalmers, J. M.; Rutten, F. J. M.; Fisher, S. E.; Symonds, I. M.; Hitchcock, A.; Allibone, R.; Dias-Gunasekara, S. *Faraday Discuss.* **2004**, *126*, 27−39.

JA044460U